APPENDIX

DROWNING OF THE TRIASSIC YANGTZE PLATFORM, SOUTH CHINA, BY TECTONIC SUBSIDENCE INTO TOXIC DEEP WATERS OF AN ANOXIC BASIN

MARCELLO MINZONI, DANIEL J. LEHRMANN, ERICH DEZOETEN, PAUL ENOS, PAUL MONTGOMERY, ADRIAN BERRY, YANJIAO QIN, YU MEIYI, BROOKS B. ELLWOOD, JONATHAN L. PAYNE

Journal of Sedimentary Research, XXXX v. XX, XXX–XXX; DOI: http://dx.doi.org/XXXXX/jsr.XXXX

Analytical Methods used in magnetic susceptibility

All materials are "susceptible" to becoming magnetized in the presence of an external magnetic field, and initial low-field bulk, mass magnetic susceptibility (M) is an indicator of the strength of this transient magnetism. MS is very different from remanent magnetism (RM), the intrinsic magnetization that accounts for the magnetostratigraphic polarity of materials. M in marine stratigraphic sequences is generally considered to be an indicator of detrital iron-containing paramagnetic and ferrimagnetic grains, mainly ferromagnesian and clay minerals (Bloemendal and deMenocal, 1989; Ellwood et al., 2008; da Silva and Boulvain, 2002, 2005), and can be quickly and easily measured on small friable samples. In the very low inducing magnetic fields that are generally applied, M is largely a function of the concentration and composition of the magnetizable material in a sample. M can be measured on small, irregular lithic fragments and on highly friable material that is difficult to sample for RM measurement.

Low-field magnetic susceptibility, as used in most reported studies, is defined as the ratio of the induced moment ($\mathbf{M_i}$ or $\mathbf{J_i}$) to the strength of an applied, very low-intensity magnetic field ($\mathbf{H_j}$), where

$$\mathbf{J_i} = \chi_{ij}\mathbf{H_j} \quad \text{(mass-specific)} \qquad (1)$$

or

$$\mathbf{M_i} = \kappa_{ij}\mathbf{H_j}. \quad \text{(volume-specific)} \qquad (2)$$

In these expressions, magnetic susceptibility in SI units is parameterized as K, indicating that the measurement is relative to a one cubic meter volume (m^3) and therefore is dimensionless;

magnetic susceptibility parameterized as M indicates measurement relative to a mass of one kg, and is given in units of m^3/kg.

Analytical Methods used in Magnetic-Reversal Stratigraphy

Figure 1 shows the magnetostratigraphy for the Upper Triassic Carnian strata at the Upper Yongningzhen (Wayao) and Longtou sections. Magnetostratigraphic data collected at Wayao and Longtou defined a series of normal and reverse magnetozones that characterize a geomagnetic polarity record for the Late Triassic. Detailed demagnetization experiments have resulted in the isolation of a Late Triassic paleomagnetic directional component. Magnetostratigraphic data from Wayao and Longtou was subjected to the "reversal test" (McFadden and McElhinny, 1990) and passed at a grade 'b' and 'c' level respectively. A sub-set of the magnetostratigraphic data from the Wayao section passed a 'fold test'. Comparison with predicted Triassic paleomagnetic directions for the Wayao locality show good agreement (derived from published paleomagnetic poles summarized by Enkin et al., 1992 and van der Voo, 1993). Comparison with predicted Triassic paleomagnetic directions for the Longtou and Gaicha localities showed poor agreement. However, the sequence of magnetic-polarity reversals in the two sections show a good correlation and are constrained by high-resolution magnetic-susceptibility profiles; it is highly likely that the magnetization observed is primary. Based on this evidence a primary paleomagnetic signal is interpreted for the Wayao and Longtou - Gaicha sections.

Sampling and Measurement

A total of 96 paleomagnetic samples were collected from 190 meters of west dipping (35-50^o) upper Triassic dark-gray, deep-water limestone using a sampling frequency of approximately 2 meters at the Wayao section. A total of 52 paleomagnetic samples were collected from 100 meters of steep, east dipping (40^o) upper Triassic light-gray, shallow water limestone using a sampling frequency of approximately 2 meters at Longtou - Gaicha section. Cylindrical samples (diameter $\approx$ 2.5 cm, length $\approx$ 6-12 cm) were cored with a portable gasoline-powered drill with a water-cooled stainless steel diamond bit. Prior to paleomagnetic samples being detached from the outcrop they were oriented using an orientation stage which determined the inclination of the core axis and a magnetic compass was used to determine the azimuth of the core axis. One sample was collected from each successive stratigraphic sampling horizon, and multiple specimens were prepared in the laboratory from each sample. Typically two paleomagnetic specimens were prepared from each sample, with demagnetization experiments initially carried out on one of the specimens. Where magnetic-polarity results were uncertain a second specimen was analyzed. Measurements of remanent magnetism were made using a 2G-755R cryogenic magnetometer with a fully automated transport system and in-line two-axis static degausser, housed in a magnetically shielded environment at the Berkeley Geochronology Center, Berkeley, California.

The NRM of all specimens were measured and were found to range from 0.025 to 35 mA/m. Stepwise demagnetization and measurement of magnetic remanence were performed on 301 specimens. Specimens were subjected to detailed alternating field (AF) and thermal demagnetization

analyses. AF demagnetization was carried out using a two-axis, stationary sample, in-line demagnetizers attached to the magnetometer with 2.5 mT demagnetization steps up to 10 mT. AF demagnetization in isolation failed to remove a recent geomagnetic-field overprint. Thermal demagnetization was carried out using a non-inductively wound ASC model TD48 resistance furnace (cooling chamber residual field ≈ 2-5 nT). The thermal demagnetization procedure, devised according to the result of rock-magnetism studies (see section on magnetic mineralogy), employed steps of 30°C between 95°C and 165°C, then 25°C up to 525°C, in combination with AF demagnetization at 10 mT. At temperatures of 95 - 125°C the NRM intensity of most samples was reduced by greater than 60%. Magnetic-susceptibility measurements using a Bartington MS-2 magnetic susceptibility bridge were made after each thermal-demagnetization step to detect mineralogical changes during heating. Interpretable magnetostratigraphic data were obtained from nearly all of the paleomagnetic samples analyzed, enabling a paleomagnetic component of Late Triassic age to be isolated.

Magnetic Mineralogy

Specimens (27) collected at regular intervals throughout Wayao section were subjected to isothermal remanent magnetization (IRM) acquisition experiments. These IRM acquisition experiments are summarized in Figure 2. Only two of the specimens became magnetically saturated at low applied magnetic fields (0.1 - 0.3 T) yielding IRM0.3T/IRM1.2T ratio values greater than 0.9. Three of the specimens yield IRM0.3T/IRM1.2T ratio values greater than 0.8 with a further three specimens yielding ratio values greater than 0.5. The remaining 19 specimens yielded IRM0.3T/IRM1.2T ratio values less than 0.5 (Fig. 2).

Thermal demagnetization of a composite three-axis IRM was employed to aid further identification of the magnetic mineralogy. An IRM was applied sequentially along three orthogonal axes of the specimens using an ASC Impulse Magnetizer and decreasing magnetizing fields of 1.2 T, 0.4 T, and 0.2 T. AF demagnetization in 10 mT increments up to 150 mT indicate a range in coercivities (Fig. 3 A i, B i & C i). Thermal demagnetization of the three orthogonal “soft”, “medium”, and “hard” IRMs , using thermal increments of 20°C to 50°C, indicated a maximum unblocking temperature of 550 - 575°C in the “medium” and “soft” IRM in the vast majority of samples (70%), with a secondary unblocking temperatures occurring at approximately 300°C (Fig. 3 A iii, B iii, C iii) in the “hard”, “medium”, and “soft” IRMs. An unblocking temperature of approximately 85°C was observed in the “hard” IRM in the vast majority of samples (70%) (Fig. 3 A iii, C iii).

Magnetic-susceptibility measurements were made after each thermal demagnetization step to detect mineralogical changes during heating and a significant increase in magnetic susceptibility was observed at temperatures above 350°C in approximately 25% of specimens (Fig. 3 B iii). Paleomagnetic thermal demagnetization experiments on typical Wayao limestone (dark gray) showed unblocking temperatures in the range of 85°C to 550°C, occasionally associated with an increase in NRM intensity and magnetic susceptibility at temperatures above 350°C.

The results of these rock-magnetism studies indicate that the typical dark-gray limestones of the Guandao section are dominated by one or two low-coercivity magnetic-mineral phases with unblocking

temperatures of ca. 300°C ("soft" and "medium" IRM) and ca. 580°C ("hard" IRM). The lower unblocking temperature of ca. 300°C is probably indicative of an iron sulfide such as pyrrhotite or a low-temperature oxidation product such as goethite, which probably formed as a result of diagenesis in the deep-water, reducing environment at the margin of the Yangtze Platform where the Wayao section limestone accumulated. Further evidence that supports the 'iron sulfide' interpretation is that an increase in the magnetic moment and magnetic susceptibility during thermal demagnetization occurs at a temperature of ca. 350°C as iron sulfide oxidizes to magnetite. The higher unblocking temperature of ca. 580°C recorded by the "soft" and "medium" IRM indicates the presence of either magnetite of low-Ti titanomagnetite (Curie temperature ca. 580°C).

The presence of pyrrhotite in the Wayao section limestone provides a significant challenge to definition of a primary ChRM direction because the high-stability paleomagnetic direction preserved by magnetite could only be defined between the temperature at which the pyrrhotite-bearing magnetic component is removed (320 - 340°C) and the temperature at which the magnetic transformation of pyrrhotite to magnetite occurs (420°C). Therefore, stepwise thermal demagnetization experiments were devised that included multiple demagnetization steps between 320 and 420°C (10 - 20°C thermal and 5 - 10 mT AF demagnetization steps). In the Wayao section, this typically resulted in higher-stability paleomagnetic directions being defined by only three demagnetization vectors. In the Longtou and Gaicha sections demagnetization was less problematic with the ChRM defined over greater temperature intervals and more demagnetization vectors. The application of field tests, such as fold and reversals test, to the demagnetization data were used to establish the primary nature of the paleomagnetic directional data defined by the thermal-demagnetization experiments (see section on reliability of paleomagnetic data).

Characteristic remanent-magnetization (ChRM) directions were identified from the demagnetization data by analyzing stereographic projections and Zijderveld diagrams ("z-plots"). ChRM directions were determined by principal component analysis (Kirschvink, 1980).

Demagnetization Behavior

During demagnetization experiments a downward-directed vector was removed during the initial thermal or AF demagnetization steps in almost all samples. In most cases this downward vector is north and corresponds approximately to the current dipole or modern field direction. In other specimens, this initial downward direction is intermediate between normal and reverse dipole field directions, suggesting the initial removal of more than one magnetic component. The initial north, downward magnetic component was typically removed at temperature between 200 and 325°C (Figs. 4, 5).

In the majority of the samples this normal polarity direction is followed by a downward southeast (Figs. 4 C, 5 C) or a upward north-west directed vector (Figs. 4 D, 5 A). These vectors were typically defined between 325 and 400°C. In some specimens of pinkish-gray limestone from Longtou these directions persisted to beyond 525°C. Application of a structural correction resulted in the downward southeast directed vector assuming an upward southeast direction. We interpret this as indicative of a reverse-polarity direction that has undergone a subsequent tectonic rotation to the west. Conversely,

application of a structural correction causes the upward northwest directed vector to assume a downward northwest direction. We interpret this as a normal-polarity direction that has been rotated to the west.

A steady decline in magnetic intensity was observed during both AF and thermal demagnetization. An unblocking temperature of ca. 85 - 125°C was observed in many samples (Figs. 4 F, 5 E) and is interpreted as removal of a paleomagnetic component probably carried by goethite. A more stable magnetic component unblocks at a temperature between 250 and 340°C and is most likely associated with the destruction of magnetic component carried by pyrrhotite (Fig. 4 E). Magnetic intensity continues to decrease and is typically reduced by 90% at temperatures of ca. 400°C. An increase in NRM intensity combined with rapidly increasing magnetic susceptibility was observed in some specimens at temperatures above 400°C. Primary paleomagnetic directional components were obtained from 301 thermally demagnetized specimens. A mean primary paleomagnetic declination of 32° and inclination of 38° (alpha 95 = 3.3°, R =189.7) for the Wayao section and a mean primary paleomagnetic declination of 4° and inclination of 48° (alpha 95 = 10.8°, R = 195.5) for the Longtou - Gaicha section was observed after structural correction.

Reliability of Paleomagnetic Data

During this study reliability criteria were adopted to provide an unbiased appraisal of the quality of the paleomagnetic data. Only stable magnetic components defined between 250°C and 700°C were used to define ChRM directions and used to define a reversal stratigraphy. Components in which over one-half the straight line segment on a z-plot was defined at a lower temperature were used only as supporting evidence for polarity definition. Directions were determined where demagnetization segments were linear, with maximum angular deviations (MAD) < 20°, and defined by three or more consecutive demagnetization vectors. Ninety-six percent of the paleomagnetic data used to define the reversal stratigraphy of this study possessed MAD values < 20°, while sixty-five percent of the data had possessed MAD values < 15°.

We consider the ChRM to be of primary origin, for the following reasons:

1. Normal and reverse directions were detected. All ChRM reverse-polarity and normal-polarity data acquired from the 301 specimens pass the reversal test (i.e., computation of mean directions, and confidence intervals about those mean directions, for both normal- and reverse-polarity groups and comparison of one mean direction with the antipode of the other direction). According to the scheme of McFadden and McElhinny (1990), the reversal test is positive (Wayao: N_{rev} = 161, N_{norm} = 55, R_{rev} = 140.83, R_{norm} = 49.54, γ_b = 8.05°; Longtou and Gaicha: N_{rev} = 48, N_{norm} = 37, R_{rev} = 41.47, R_{norm} = 35.20, γ_c = 10.29°). Passage of the reversal test indicates that the ChRM directions are free of secondary NRM components and that the paleomagnetic data have adequately averaged secular variation. Since the sets of normal and reversed-polarity sampling sites conform to stratigraphic layering, the ChRM direction is probably primary.

2. The paleomagnetic directional data from the Wayao section ($D_{mean\ WY}$ = 31.9°, $I_{mean\ WY}$= 37.7°, α95 = 3.33°, R = 189.69, k = 8.17, N = 216) are in general agreement with predicted Upper Triassic

paleomagnetic directions for the Wayao and Longtou - Gaicha localities based on published Lower Triassic paleomagnetic poles for the South China Block (SCB) (summarized by Enkin et al.,1992 and Van der Voo, 1993). The paleomagnetic directional data from the Longtou - Gaicha section ($D_{mean\ LTG\ \&\ GH}$ = 3.7°, $I_{mean\ LTG\ \&\ GH}$ = 47.7°, α95 = 10.9°, R = 41.47, k = 1.93, N = 85) is in general agreement with respect to the inclination reported by Enkin et al. (1992) but not the declination (Table 1).

We conclude from the outcome of these comparisons that the Lower Triassic ChRM direction from Wayao section is the same as the predicted Triassic paleomagnetic direction based on previously published paleomagnetic poles and therefore the ChRM defined in this study is primary.

3. The high-stability ChRM defined at temperatures between 300 and 580°C and above is carried by stable magnetite (or low-Ti Titanomagnetite) (Fig. 3). We conclude from the outcome of these tests that the Lower Triassic ChRM direction from Wayao and Longtou - Gaicha is recorded by magnetite and has a paleomagnetic direction similar to the predicted Upper Triassic paleomagnetic direction based on previously published paleomagnetic poles. Therefore the ChRM defined from the higher-unblocking-temperature magnetic components (> 300°C) is primary.

4. In the majority of samples the NRM and low-stability magnetic overprint is carried by minerals with low coercivity (up to 15 mT) and low unblocking temperatures (< 300°C) (Fig. 3). Prior to structural correction this magnetic component has a direction that is different from the ChRM carried by more stable magnetic minerals in the same rock but similar to the present-day direction of the geomagnetic field at Wayao and Logtou - Gaicha locations ($D_{present\ day}$ = 9°, $I_{present\ day}$ = 44°). We can conclude that the low-stability magnetic overprint was acquired post - folding of the Wayao and Longtou - Gaicha sections and its similarity with the present-day field direction indicates that it was acquired relatively recently.

5. Structural corrections (fold test) applied to the a subset of ChRM data (26 samples) from the Wayao section results in an improvement in the directional sense and clustering of the ChRM defined from the Wayao section (Fig. 6), indicating that the most stable magnetic component was acquired prior to folding. Though all the ChRM data come from one locality, the bedding tilts are sufficiently different for this result to constitute a statistically significant passage of the bedding tilt test at a significance level of 99% (i.e., for the Wayao section limestone, N = 26, k_{before} = 2.86, k_{after} = 8.16, and k_{after}/k_{before} = 2.86). The degrees of freedom are 2(N-1) = 50, and the F-distribution value $F_{50,50}$ for 1% significance level is ca. 2. With the ratio $k_{after}/k_{before} > F_{50,50}$ the improvement in grouping produced by applying a structural correction is significant at the 1% level). Since it has been shown that the structural correction results in a significant reduction in dispersion of the site-mean ChRM direction, it can be concluded that the magnetostratigraphy pre-dates the time of folding (i.e., pre - Late Cretaceous (Opdyke et al., 1986).

6. The identification of a closely similar stratigraphic pattern of magnetization in the Wayao and Longtou - Gaicha sections (Fig. 7) that are essentially the same age, widely separated and in different rock types (deep and shallow water carbonates) suggests that the magnetism is stable, and dates from the time of deposition. Since a given sequence of magnetic polarity reversals can be identified in each of

the two sections and there is a good match in the sequence between the sections, constrained by high-resolution magnetic susceptibility profiles, then it is highly likely the magnetization observed is primary.

Magnetostratigraphic Results

The magnetic polarity of the ChRM, defined by incremental-demagnetization studies, is plotted, together with declination, inclination, and the virtual geomagnetic polar latitudes (VGP) for the Wayao and Longtou - Gaicha sections are summarized in Figure 1. Declination, inclination, and VGP latitude are corrected for the tectonic rotations observed at the Wayao and Longtou-Gaicha localities. This correction was achieved by calculating the difference in declination and inclination between the site-mean ChRM and the site geomagnetic-field direction as predicted by the geocentric axial dipole model, and rotating declination and inclination of each sample site ChRM by the calculated difference.

The definition of the magnetic polarity is based on VGP latitude. South VGP latitudes (negative) are interpreted as reverse polarity whereas north VGP latitudes (positive) are interpreted as normal. In Figure 6 the magnetozone definition is based on a minimum of two consecutive specimens exhibiting the same polarity and MAD values less than 20^{o} (n = 220). Individual specimens that show opposite polarity to adjacent specimens are indicated by half bars in the magnetic-polarity column of Figure 2. The remaining 23 interpretable specimens (MAD > 20^{o}) were used to better define magnetozone boundaries. Ten normal-polarity and ten reverse-polarity magnetozones were defined during this study.

References

Bloemendal, J., and deMenocal, P., 1989, Evidence for a change in the periodicity of tropical climate cycles at 2.4 Myr from whole-core magnetic susceptibility measurements: Nature, v. 342, p. 897-900.

da Silva, A-C., and Boulvain, F., 2002, Sedimentology, magnetic susceptibility and isotopes of a Middle Frasnian carbonate platform: Tailfer Section, Belgium: Facies v. 46, p. 89-102.

da Silva, A.-C., and Boulvain, F., 2005. Upper Devonian carbonate platform correlations and sea level variations recorded in magnetic susceptibility: Palaeogeography, Palaeoclimatology, Palaeoecology, v. 240, p. 373-388.

Ellwood, B.B., Tomkin, J.H., Ratcliffe, K.T., Wright, M., and Kafafy, A.M., 2008, High resolution magnetic susceptibility and geochemistry for the Cenomanian / Turonian boundary GSSP with correlation to time equivalent core: Palaeogeography, Palaeoclimatology, Palaeoecology, v. 261, p. 105-126.

Enkin R.J., Zhenyu Y., Yan C., and Courtillot V., 1992, Paleomagnetic constraints on the geodynamic history of the major blocks of China from the Permian to the present: Journal of Geophysical Research, v. 97, p. 13,953–13,989.

Kirschvink, J.L., 1980, The least-squares line and plane and analysis of paleomagnetic data: Geophysical Journal International, v. 62, 699-718.

Lowrie, W., 1990, Identification of ferromagnetic minerals in a rock by coercivity and unblocking temperature properties:Geophysical Research Letters, v. 17, 159-162.

McFadden, P.L. and McElhinny, M.W., 1990, Classification of the reversal test in paleomagnetism, Geophysical Journal International, v. 103, 725-729.

Opdyke, N.D., Huang, K., Xu, G., Zhang, W. Y., and Kent, D.V. , 1986, Paleomagnetic results from the Triassic of the Yangtze Platform, Journal of Geophysical Research, v. 91, 9553-9568.

Vander Voo, R., 1993, Paleomagnetism of the Atlantic, Tethys and Iapetus oceans: Cambridge University Press, Cambridge, 411 p.

Figure Captions

Table 1: Comparison of predicted paleomagnetic directions derived from the paleopole published by Enkin et al. (1992) and Van der Voo (1993) and the measured Triassic directions from this study for the Wayao, Longtou-Giacha sections.

Fig 1. – Magnetostratigraphic results from the **A)** Wayao and **B)** Longtou - Gaicha section. From right to left, the diagram shows height, declination, inclination, VGP latitude of the ChRM of all data that meet the reliability criteria defined in the text, magnetic polarity, maximum angle of deviation (MAD), number of demagnetization vectors that define the ChRM, and demagnetization temperature range that defined the ChRM. Normal polarity is indicated by black and reverse polarity by white in the magnetic polarity column. Half bars in the magnetic polarity column indicate individual specimens that show opposite polarity to adjacent specimens.

Fig 2. – Curves of isothermal remanent magnetization (IRM) for 27 representative limestone samples from the Wayao section. Plot shows normalized acquired remanence against applied magnetic field.

Fig 3. – Typical IRM acquisition and thermal-demagnetization behavior for three representative samples of limestone from the Wayao section (WY2, WY87, and WY61). From top to bottom curves show: **Ai), Bi) and Ci)** Normalized IRM against demagnetization field (mT) and applied field (T). Normalized IRM acquisition is shown in blue and AF demagnetization is shown in dark green. **Aii), Bii) and Cii)** Normalized IRM against thermal-demagnetization temperature (^{o}C) and applied field (T). Normalized IRM acquisition is shown in blue, and thermal demagnetization of the IRM is shown in red. **Aiii), Biii) and Ciii)** Normalized IRM against thermal demagnetization of three orthogonal components (0.02T (orange line), 0.2 - 0.4 T (dark blue line), and 0.4 - 1.2 T (light green line)). **Aiv), Biv) and Civ)** Normalized IRM against magnetic susceptibility and against demagnetization temperature (^{o}C). Magnetic susceptibility after each thermal-demagnetization step is also plotted in orange, and thermal demagnetization of the IRM is shown in red. **Example A)** consists of a specimen of light-gray dolomitized limestone and exhibits three unblocking temperatures at 85^{o}C, 300^{o}C, and 575^{o}C. The lowest unblocking temperature results in the removal of the hard IRM. The most stable (soft, medium) IRM is removed between 300^{o}C and 575^{o}C. Magnetic susceptibility remains low and relatively constant up to a temperature of 700^{o}C. **Example B)** consists of a specimen of dark-gray deep-water limestone and exhibits two unblocking temperatures at 300^{o}C and 575^{o}C. The lower unblocking temperature results in the removal of the soft and medium IRM. The most stable (hard) IRM is removed at 575^{o}C. However, magnetic susceptibility begins to rise at

temperatures between 300 and 400°C, indicating the formation of new magnetic mineral phases. As the temperature rises above 400°C, susceptibility rises significantly. **Example C)** consists of a specimen of dark-gray deep-water limestone and exhibits three unblocking temperatures at 85°C, 300°C and 575°C. The lowest unblocking temperature results in the removal of the hard IRM. The most stable (soft, medium) IRM is removed between 300°C and 575°C. Magnetic susceptibility remains low and relatively constant up to a temperature of 700°C.

Fig 4. – Examples of typical demagnetization experiments on specimens collected from the Wayao section. **A)** Reverse-polarity sample WY20-X, collected at a stratigraphic height of 48.7 m. **B)** Reverse-polarity sample WY45A-X, collected at a stratigraphic height of 99.7 m. **C)** Reverse-polarity sample WY48-C, collected at a stratigraphic height of 106.25 m. **D)** Normal-polarity sample WY94-C, collected at a stratigraphic height of 186.95 m. **E)** Normal-polarity sample WY46-TAF, collected at a stratigraphic height of 102 m. **F)** Normal-polarity sample WY72-D, collected at a stratigraphic height of 148.25 m. The figures show from left to right: z-plot of demagnetization in stratigraphic coordinates; filled circles are projections of vectors onto the horizontal plane with north oriented to the top; open circles are projections onto a north-south vertical plane and equal-area stereographic projection of demagnetization vectors in stratigraphic coordinates.

Fig 5. – Examples of typical demagnetization experiments on specimens collected from the Longtou-Gaicha sections. **A)** Normal-polarity sample GH2-B, collected at a stratigraphic height of -12 m in the Gaicha section. **B)** Reverse-polarity sample LTG3-A, collected at a stratigraphic height of 10.5 m in the Longtou section. **C)** Reverse-polarity sample LTG8-A, collected at a stratigraphic height of 19 m in the Longtou section. **D)** Normal-polarity sample LTG21-A, collected at a stratigraphic height of 43.75 m in the Longtou section. **E)** Reverse-polarity sample LTG10-B, collected at a stratigraphic height of 23 m in the Longtou section. **F)** Reverse-polarity sample LTG43-A, collected at a stratigraphic height of 79.6 m in the Longtou section. The figures show from left to right: z-plot of demagnetization in stratigraphic coordinates; filled circles are projections of vectors onto the horizontal plane with north oriented to the top; open circles are projections onto a north-south vertical plane and equal-area stereographic projection of demagnetization vectors in stratigraphic coordinates.

Fig 6. – Results of a "fold test" carried out on a small parasitic fold from Wayao section (at 88-102 m in section). **A)** equal-area stereographic projection of demagnetization vectors in geographic coordinates, and **B)** equal-area stereographic projection of demagnetization vectors in stratigraphic coordinates. An improvement in the directional sense and clustering of the ChRM defined from the Wayao section (Fig. 6) indicates that the most stable magnetic component was acquired prior to folding. This stability test represents a statistically significant passage of the bedding tilt test at a significance level 99%. Since it has been shown that the structural correction results in a significant reduction in dispersion of the site mean ChRM direction, it can be concluded that the magnetostratigraphy predates the time of folding.

Fig 7. – Correlation between Longtou - Gaicha and Wayao sections using magnetostratigraphy and magnetic-susceptibility profile.

Table 1.

LOCATION	REFERENCE POLE	AGE	PREDICTED			THIS STUDY		
			DEC.	INC.	A95	DEC.	INC.	A95
WAYAO	ENKIN, 1992	T2-T3	48°	34°	16.8°	32°	38°	3.3°
WAYAO	VAN DER VOO, 1993	TU	43°	17°	11°			
GIACHA	ENKIN, 1992	T2-T3	49°	36°	16.8°	4°	48°	11°
GIACHA	VAN DER VOO, 1993	TU	43°	19°	11°			
LONGTOU	ENKIN, 1992	T2-T3	48°	35°	16.8°			
LONGTOU	VAN DER VOO, 1993	TU	43°	19°	11°			

(A)

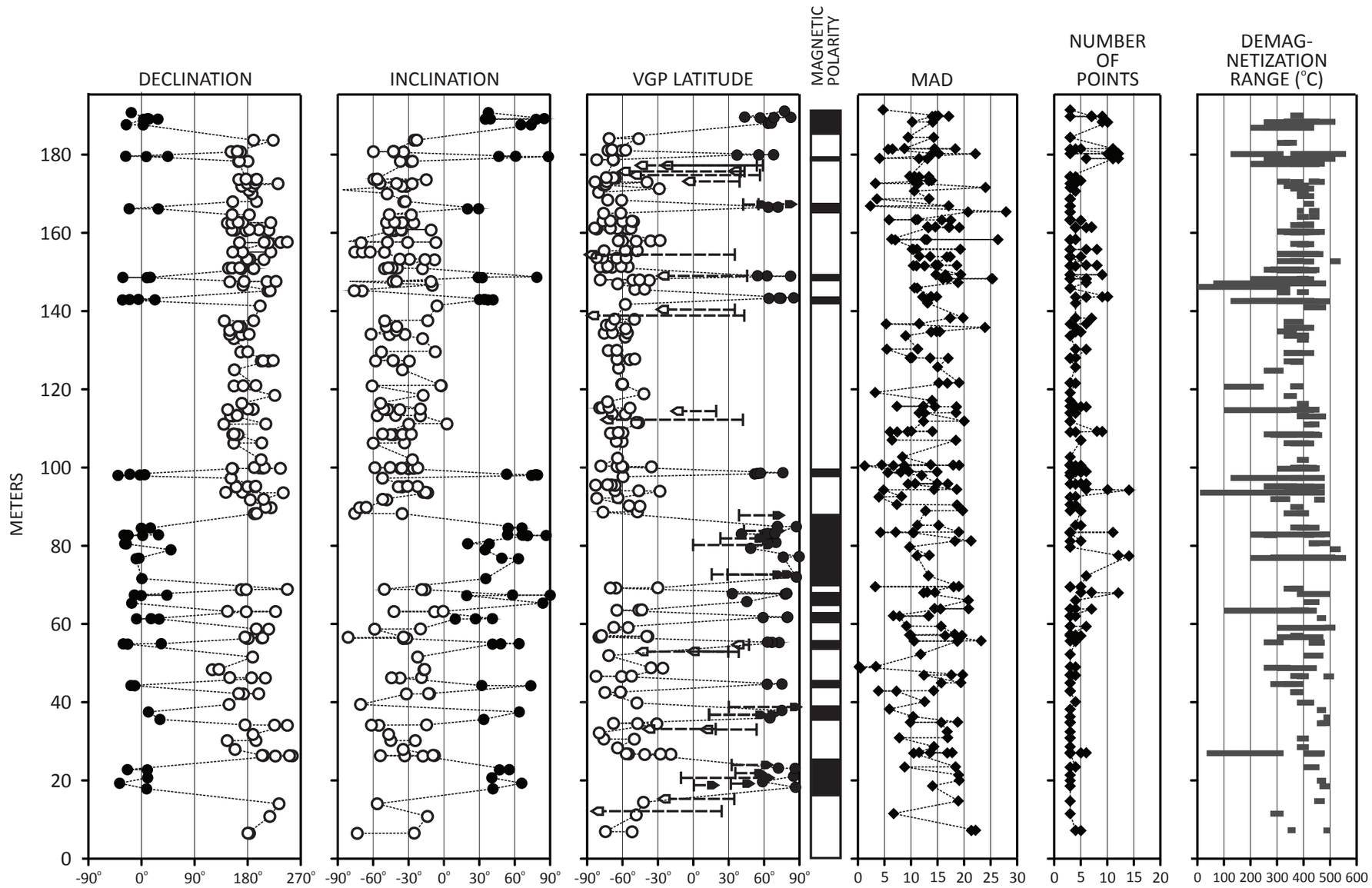
DECLINATION
INCLINATION
VGP LATITUDE
MAGNETIC POLARITY
MAD
NUMBER OF POINTS
DEMAG-NETIZATION RANGE (°C)
METERS
0
20
40
60
80
100
120
140
160
180
-90° 0° 90° 180° 270°
-90° -60° -30° 0° 30° 60° 90°
-90° -60° -30° 0° 30° 60° 90°
0 5 10 15 20 25 30
0 5 10 15 20
0 100 200 300 400 500 600

(B)

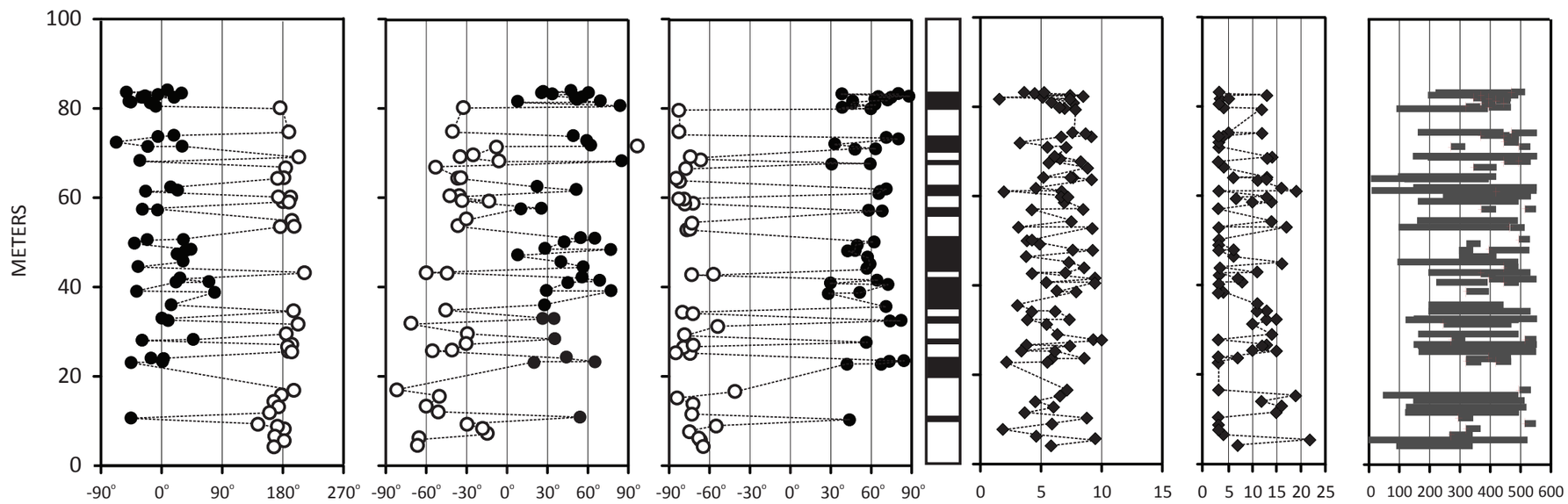
METERS
0
20
40
60
80
100
-90° 0° 90° 180° 270°
-90° -60° -30° 0° 30° 60° 90°
-90° -60° -30° 0° 30° 60° 90°
0 5 10 15
0 5 10 15 20 25
0 100 200 300 400 500 600

Figure 1

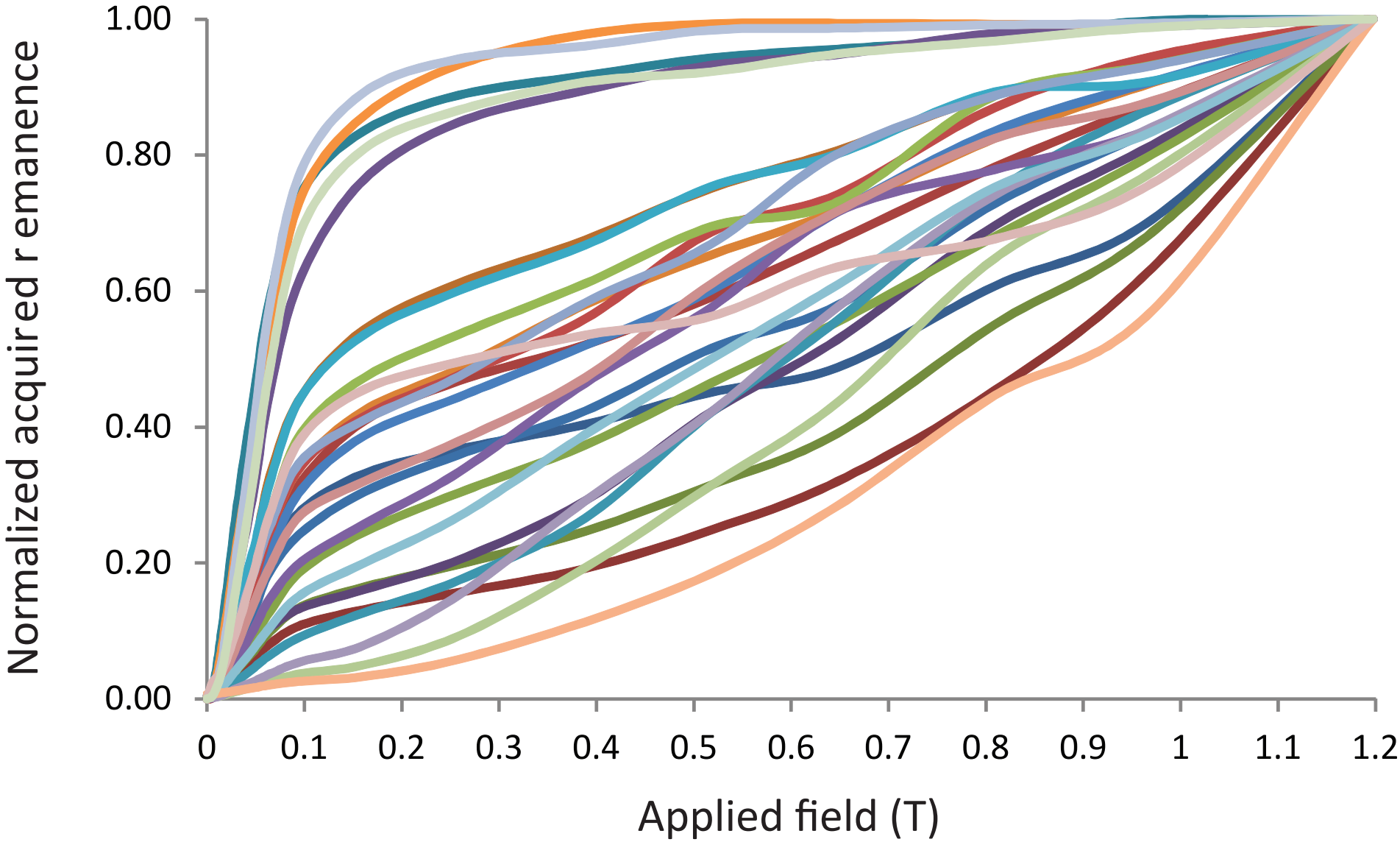
Normalized acquired r emanence
1.00
0.80
0.60
0.40
0.20
0.00
0
0.1
0.2
0.3
0.4
0.5
0.6
0.7
0.8
0.9
1
1.1
1.2
Applied field (T)

Figure 2

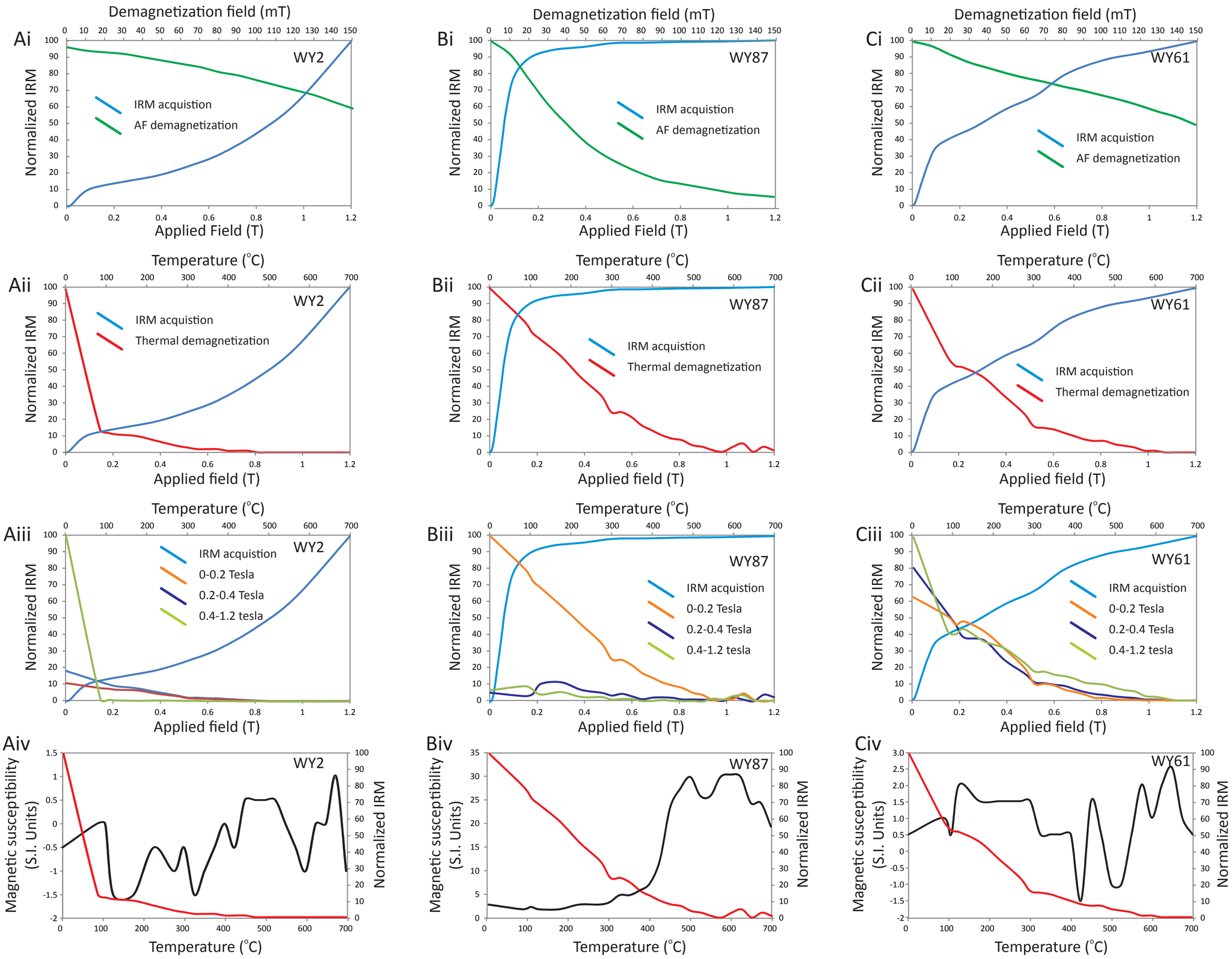
Ai
Demagnetization field (mT)
WY2
IRM acquistion
AF demagnetization
Normalized IRM
Applied Field (T)
Bi
WY87
Ci
WY61
Aii
Temperature (°C)
Thermal demagnetization
Bii
Cii
Aiii
0-0.2 Tesla
0.2-0.4 Tesla
0.4-1.2 tesla
Applied field (T)
Biii
Ciii
Aiv
Magnetic susceptibility (S.I. Units)
Biv
Civ

Figure 3

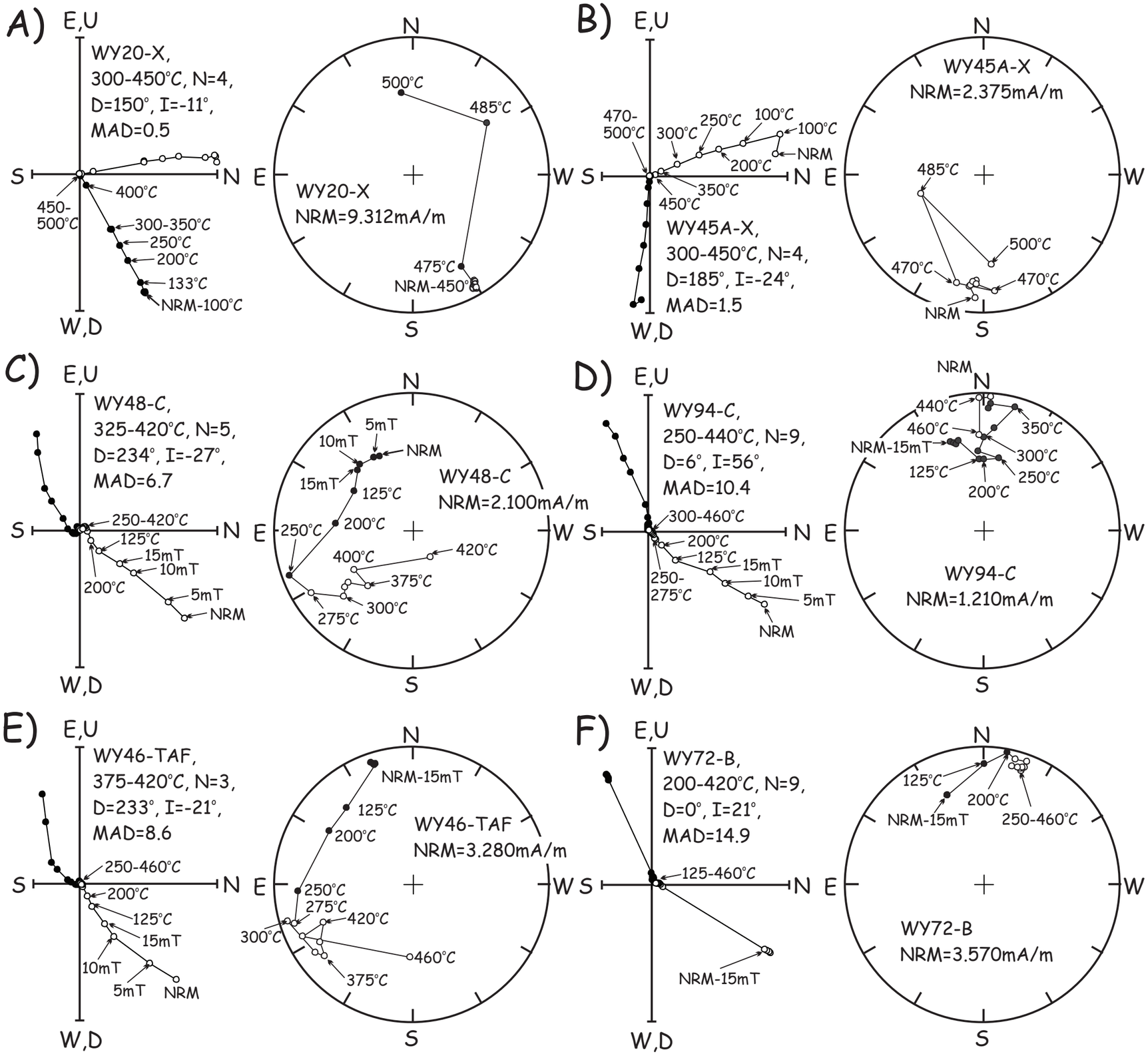

S = south N=north W,D = west, down E,U = east, up Horizontal plane, lower hemisphere Vertical plane, upper hemisphere

Figure 4

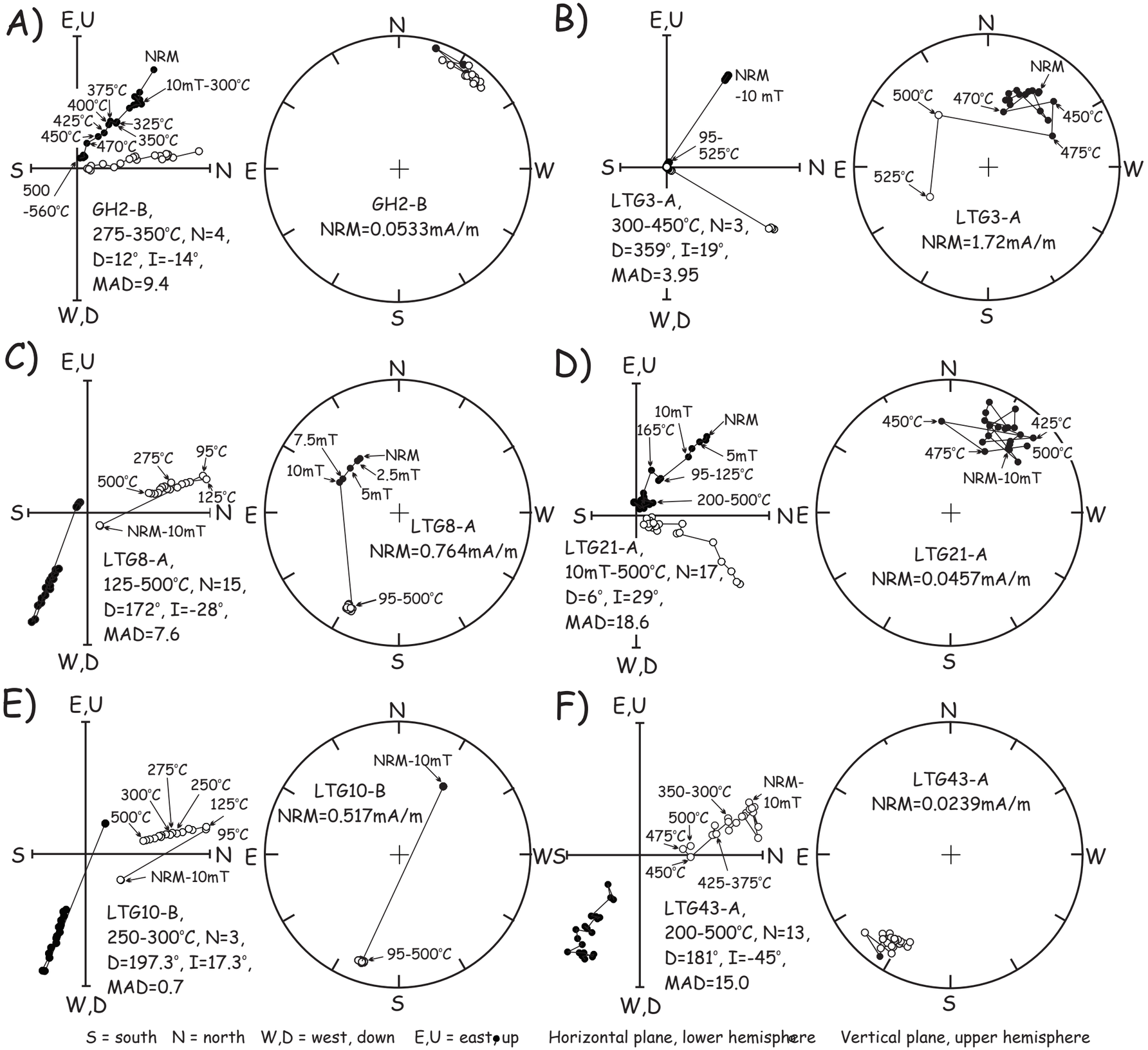
A)
E,U
NRM
10mT-300°C
375°C
400°C
425°C
450°C
325°C
350°C
470°C
S
N
500
-560°C
W,D
GH2-B,
275-350°C, N=4,
D=12°, I=-14°,
MAD=9.4
N
E
W
S
GH2-B
NRM=0.0533mA/m
B)
E,U
NRM
-10 mT
95-
525°C
S
N
LTG3-A,
300-450°C, N=3,
D=359°, I=19°,
MAD=3.95
W,D
N
NRM
500°C
470°C
450°C
475°C
525°C
E
W
S
LTG3-A
NRM=1.72mA/m
C)
E,U
275°C
95°C
500°C
125°C
S
N
NRM-10mT
LTG8-A,
125-500°C, N=15,
D=172°, I=-28°,
MAD=7.6
W,D
N
7.5mT
NRM
10mT
2.5mT
5mT
E
W
LTG8-A
NRM=0.764mA/m
95-500°C
S
D)
E,U
10mT
165°C
NRM
5mT
95-125°C
200-500°C
S
NE
LTG21-A,
10mT-500°C, N=17,
D=6°, I=29°,
MAD=18.6
W,D
N
450°C
425°C
475°C
500°C
NRM-10mT
W
LTG21-A
NRM=0.0457mA/m
S
E)
E,U
275°C
300°C
250°C
125°C
500°C
95°C
S
N
NRM-10mT
LTG10-B,
250-300°C, N=3,
D=197.3°, I=17.3°,
MAD=0.7
W,D
N
NRM-10mT
LTG10-B
NRM=0.517mA/m
E
W
95-500°C
S
F)
E,U
350-300°C
NRM-
10mT
500°C
475°C
450°C
425-375°C
WS
N
E
LTG43-A,
200-500°C, N=13,
D=181°, I=-45°,
MAD=15.0
W,D
N
LTG43-A
NRM=0.0239mA/m
W
S
S = south N = north W,D = west, down E,U = east, up
Horizontal plane, lower hemisphere
Vertical plane, upper hemisphere

Figure 5

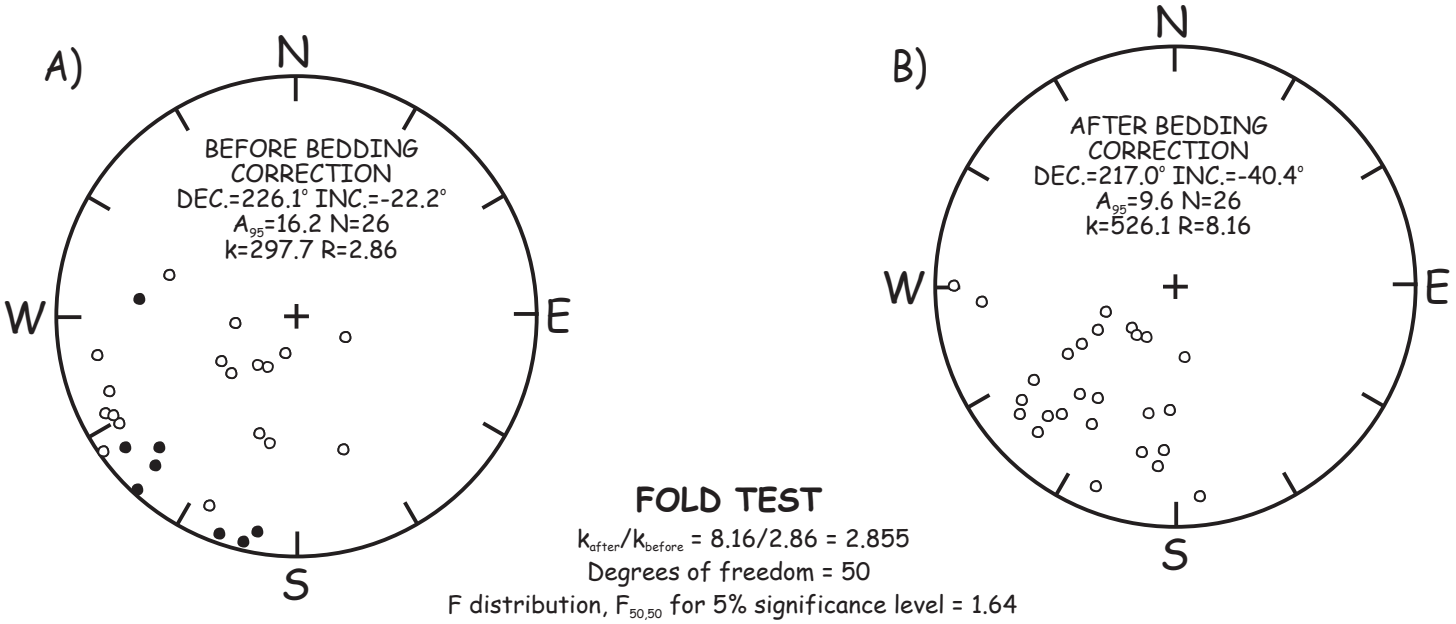

FOLD TEST

k_{after}/k_{before} = 8.16/2.86 = 2.855

Degrees of freedom = 50

F distribution, $F_{50,50}$ for 5% significance level = 1.64

F distribution, $F_{50,50}$ for 2.5% significance level = 1.81

F distribution, $F_{50,50}$ for 1% significance level = 2.02

k_{after}/k_{before}(2.855) > $F_{50,50}$ for 1% sig. level (2.02)

Figure 6

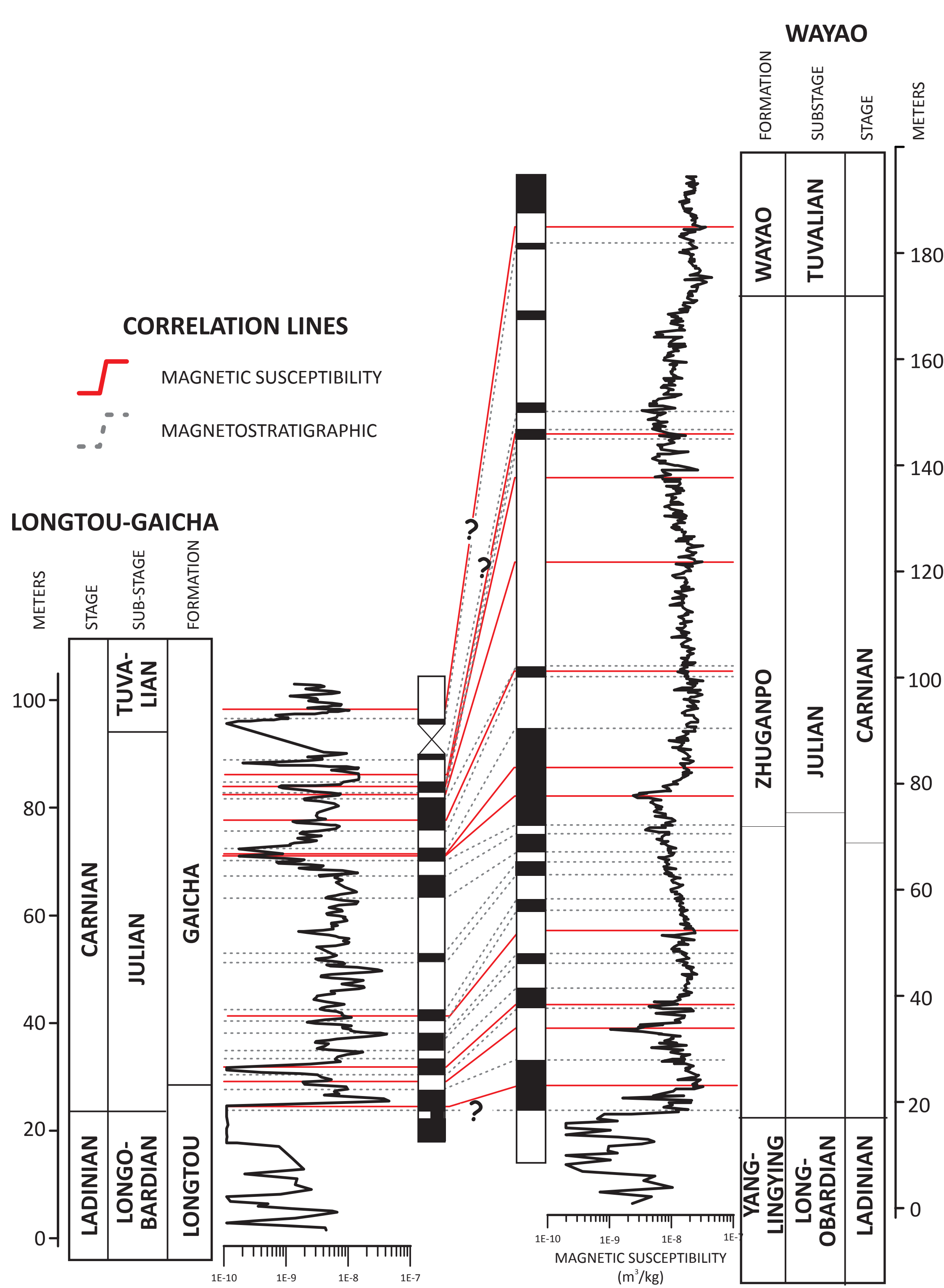
CORRELATION LINES
MAGNETIC SUSCEPTIBILITY
MAGNETOSTRATIGRAPHIC
LONGTOU-GAICHA
METERS
STAGE
SUB-STAGE
FORMATION
100
80
60
40
20
0
CARNIAN
TUVA-LIAN
JULIAN
LADINIAN
LONGO-BARDIAN
LONGTOU
GA
1E-10
1E-9
1E-8
1E-7
MAGNETIC SUSCEPTIBILITY
(m3/kg)
WAYAO
FORMATION
SUBSTAGE
STAGE
METERS
WAYAO
TUVALIAN
ZHUGANPO
JULIAN
CARNIAN
YANG-LINGYING
LONG-OBARDIAN
LADINIAN
180
160
140
120
100
80
60
40
20
0
1E-10
1E-9
1E-8
1E-7
MAGNETIC SUSCEPTIBILITY
(m3/kg)

Figure 7